Received 4 July 2018; revised 29 August 2018; accepted 18 September 2018. Date of publication 24 September 2018;
date of current version 1 March 2019. The review of this paper was arranged by Editor S. Reggiani.

Digital Object Identifier 10.1109/JEDS.2018.2872037

Effects of Interface States on Ge-On-SOI Photodiodes

CHONG LI [1], BEN LI[1], SHIHONG QIN[1], JIALE SU[1], XIAOYING HE [2], AND XIA GUO [2]

1 Department of Information, Beijing University of Technology, Beijing 100124, China
2 School of Electronic Engineering, Beijing University of Posts and Telecommunications, Beijing 100876, China

CORRESPONDING AUTHOR: C. LI (e-mail: lichong@bjut.edu.cn)

This work was supported in part by the Natural National Science Foundation of China under Grant 61505003, Grant 61675046, and Grant 61335004, and in part by the National Key Research and Development Program of China under Grant 2016YFB0400603, Grant 2017YFB0400902, and Grant 2017YFF0104801.

ABSTRACT The 4.2% mismatch at the Si/Ge interface has a significant impact on Si/Ge photodetectors. However, few researchers have attempted to determine the major noise source or study the effects of the Si/Ge interface on the dark current, the responsivity and the 3-dB bandwidth of these devices. In this letter, we found that the dark current was dominated by generation-recombination processes that were enhanced by trap-assisted-tunneling around the interface below 220 K, with a characteristic tunneling energy of $E_{00} = 14$ meV corresponding to an effective mass of $m^* = 18m_0$. This behavior can be explained by the rise in the heavy-hole band caused by the compressive strain on the Ge layer. When the temperature increased above 240 K, Shockley-Read-Hall recombination was clearly observed and believed to be dominant. The responsivity, the collection efficiency and the absorption efficiency were all extracted at 850 nm, 1310 nm, and 1550 nm. The absorption coefficient around the interface was found to be lower than that of the bulk material. In addition, comparison of the measured 3-dB frequency (~20.6 GHz @ −0.5 V) with the theoretical value (~29.37 GHz) indicated that defects have little effect on the bandwidth at high frequencies.

INDEX TERMS Photodetector, germanium.

I. INTRODUCTION

Germanium-on-silicon (Si/Ge) photodiodes are important building blocks in silicon photonics-based sensing, communications and optical interconnections at 1550 nm and 1310 nm because of their low cost and their complementary metal-oxide-semiconductor (CMOS) compatibility [1]. In addition, as CMOS-compatible photodiodes, Si/Ge photodiodes are key components for photonically-enabled application-specific integrated circuits (ASICs). The monolithic photonic integration modules and products with Si/Ge photodiodes have been fabricated by Intel and IBM [2]–[4]. However, there is a well-known 4.2% lattice mismatch between Ge and Si that causes high-density point dislocations at the interface between Ge and Si layers and threading dislocations in Ge epitaxial layers [5]–[7]. Therefore, during initial development, the silicon layer was used only as a substrate layer, and photodiodes were fabricated in the Ge material without the Si/Ge material interface [8], [9]. However, with recent advances in Ge epitaxial technology, Si/Ge heterojunction photodiodes that use the Si layer as both substrate and contact layer have been extensively used and researched [9]–[17]. Among the available Si/Ge heterojunction photodiodes, the vertical p+(Ge)-i(Ge)-n+(Si) heterojunction photodiode structure has been widely researched and used to construct high-speed photodetectors with promising device performance levels [18]–[21]. However, because of the high point dislocation density that occurs at the interface, the generation-recombination current is greatly enhanced by trap-assisted tunneling at the Si/Ge interface (J_{inter}). Additionally, because of the lower Ge bandgap, the generation-recombination current governed by the Shockley-Read-Hall (SRH) process (J_{SRH}) in Si/Ge photodiodes is higher than that in III–V photodetectors [22], [23]. Therefore, the dark current in a vertical p+(Ge)-i(Ge)-n+(Si) photodiode (44.1 mA/cm^2) is significantly higher than that in commercial III–V photodetectors (15.2 μA/cm^2) [24]. However, there have been no reports to date of determination of the major noise source or consideration of the effects of

interface states on the responsivity and 3-dB bandwidth of Si/Ge photodetectors.

In this letter, the interface effects on the dark current density in a vertical p+(Ge)-i(Ge)-n+(Si) on SOI (silicon-on-insulator) substrate photodiode are presented. The ideality factors and activation energies are then used to analyze the dark current and identify the major noise source. Next, the light currents at different input powers, wavelengths and 3-dB bandwidths are measured at 1550 nm and the effects of the interface on these currents are analyzed.

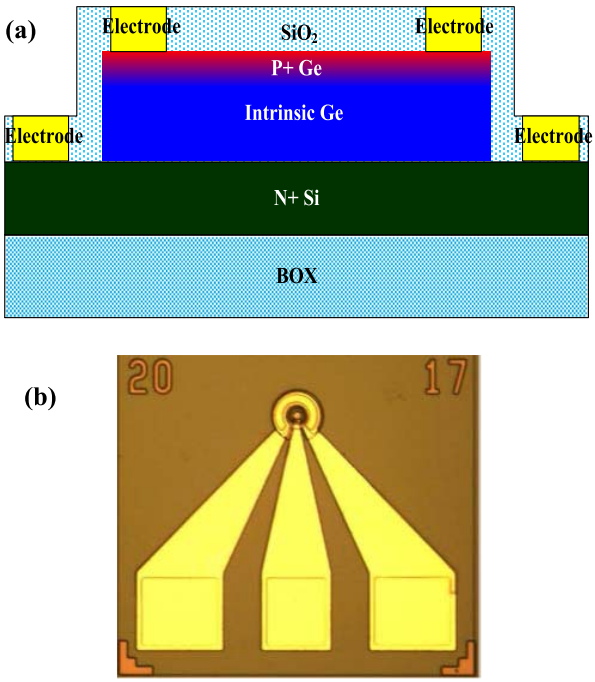

FIGURE 1. (a) Schematic of cross-section of vertical p+(Ge)-i(Ge)-n+(Si) photodetector. (b) Top view of 20-μm-diameter Si/Ge photodetector.

II. STRUCTURE

A schematic of the detector's cross-section is shown in Fig. 1(a). A SOI substrate with a 2.0-μm-thick buried oxide layer and 1.0-μm-thick highly-phosphorus-doped Si (phosphorus-doped concentration: N_p: $\sim 6 \times 10^{19}/\text{cm}^3$) layer was chosen to reduce the radio-frequency losses. A Ge film was deposited on the SOI wafer by ultra-high-vacuum chemical vapor deposition (UHV-CVD) [25]. Mesa structures with 15 μm, 18 μm, 20 μm, 25 μm, 30 μm, and 40 μm diameters were then etched [25].

III. DARK CURRENT ANALYSIS

The dark current (I_{dark}) is a superposition of six major individual current mechanisms: (1) the diffusion current (I_{diff}), (2) the generation-recombination current governed by the SRH process (I_{SRH}), where recombination occurs in the bulk semiconductor, (3) the generation-recombination current enhanced by trap-assisted-tunneling at the Si/Ge layer interface (I_{inter}), (4) the band-to-band tunneling current (I_{btb}), (5) the avalanche current (I_{ava}) that occurs under high electric fields, and (6) the shunt resistance current (I_{shunt}). The dark current (I_{dark}) is the sum of the above mechanisms:

$$I_{dark} = I_{diff} + I_{SRH} + I_{inter} + I_{btb} + I_{ava} + I_{shunt} \quad (1)$$

where I_{btb} and I_{ava} are generated at electric fields $>3 \times 10^5$ V/cm [22], which corresponds to a working voltage of more than -21 V for our devices. I_{shunt} is given by $I_{shunt} = V/R_s$; the shunt resistance (R_s) is generally approximately $10^{11}\,\Omega$ and I_{shunt} is thus negligible here [26]. Therefore, the main dark current components are I_{diff}, I_{SRH}, and I_{inter}, as illustrated in Fig. 2.

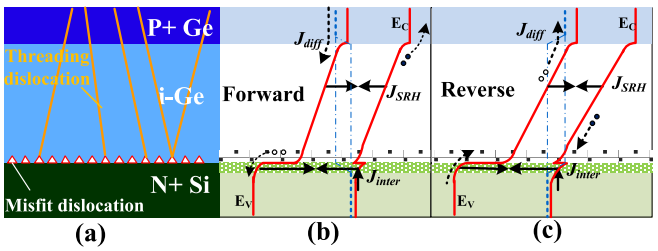

FIGURE 2. (a) Schematic diagram illustrating the dislocation distribution. Band diagrams (b) under forward bias and (c) under reverse voltage bias, showing the possible dark current sources: the diffusion current (J_{diff}.), the generation-recombination current governed by the SRH process (J_{SRH}), and the generation-recombination current enhanced by trap-assisted-tunneling J_{inter}.

The ideality factor (n) under forward bias and the activation energy (E_a) under reverse bias are generally used to analyze and differentiate these current sources [27]–[29].

1) I_{diff} is caused by thermally generated minority carriers, which are initially located inside the quasi-neutral regions, diffusing across the junction to maintain charge neutrality. In diffusion-limited diodes, the ideality factor under forward bias is $n_{diff} = 1$ [30], and the activation energy under reverse bias is $E_{a\text{-}diff} = E_g$ [31].
2) For the SRH process-limited current, the ideality factor under forward bias is $n_{SRH} = 2T^*/(T + T^*)$, where T^* is the characteristic temperature related to the defect distribution in the bandgap of the bulk material [32], and the activation energy under reverse bias is $E_{a\text{-}SRH} = E_g/2$ [33].
3) The ideality factor of I_{inter} is $n_{trap} = \frac{E_{00}}{k_B T} coth(\frac{E_{00}}{k_B T})$, where E_{00} is the characteristic tunneling energy and k_B is the Boltzmann constant. In addition, the activation energy under reverse bias $E_{a\text{-}trap} < E_g/2$ [34], as determined based on the impurity energy level and the doping concentration.

Therefore, dark currents at different temperatures in our 20-μm-measured-diameter device were measured using an Agilent B1550A semiconductor device parameter analyzer and a probe station integrated with a LakeShore temperature controller; the results are shown in Fig. 3(a). The measurement current is limited above 10^{-11} A because of the minimum perturbation error of the probe station.

The ideality factor was determined using the formula $n = \frac{q}{k_B T}\frac{V_{i+1}-V_i}{\ln I_{i+1}-\ln I_i}$ under forward bias [35], and was indicated to be a function of temperature by the diamond points shown in Fig. 3(b). In the 100–280 K range, the ideality factor is greater than n_{diff}, meaning that the diffusion current is not the major noise source. Function curves of n_{SRH} and n_{trap} were used to fit the n-T curve. At temperatures lower than 220 K, the n-T curve coincides with the curve of $n = \frac{E_{00}}{k_B T} coth(\frac{E_{00}}{k_B T})$, where $E_{00} = 14$ meV (or $E_{00}/k = 162.46$ K), thus indicating that the dark current is dominated by the generation-recombination current enhanced by trap-assisted-tunneling at the interface. Here, E_{00} is dependent on the p+ Si layer's doping concentration and the effective masses of the carriers in our diode, i.e., $E_{00} = \frac{\hbar}{2}\sqrt{\frac{N_p}{m^*\varepsilon}}$ [36], and the effective mass is $m* = 18m_0$. This can be explained using band structure theory for compressively stressed Ge. The Ge layers around the interface are initially compressively strained by the silicon layer, causing the valence sub-bands to split; here, the top of the valence band is the heavy-hole band. The heavy-hole band energy increases and the effective masses are consequently enlarged. When the temperature exceeds 240 K, the n-T curve coincides with the curves of $n = 2T^*/(T+T^*)$, and thus the dark current is dominated by the SRH process. Here, T^* is equal to 359.7 K, corresponding to a characteristic energy $E* = kT*$ equal to 31 meV, and the defect density energy distribution is determined using $N_T(E) \propto \exp(2E/E^*)$ [37].

The activation energy (E_a) was found using $I_{dark} \propto exp(-E_a/kT)$. Therefore, E_a is the slope of the function curve of the I_{dark} vs. $1000/T$ plot shown in Fig. 3(c). The activation energy is shown as a function of reverse bias voltage in Fig. 3(d) and is lower than $E_g/2$, which means that the generation-recombination current enhanced by trap-assisted tunneling at the interface is the major source of the dark current under reverse bias. Because the tunneling probability is dependent on the barrier width, the generation-recombination current enhanced by trap-assisted tunneling increases exponentially with increasing reverse bias voltage, while the activation energy decreases with increasing voltage, as shown in Fig. 3(d).

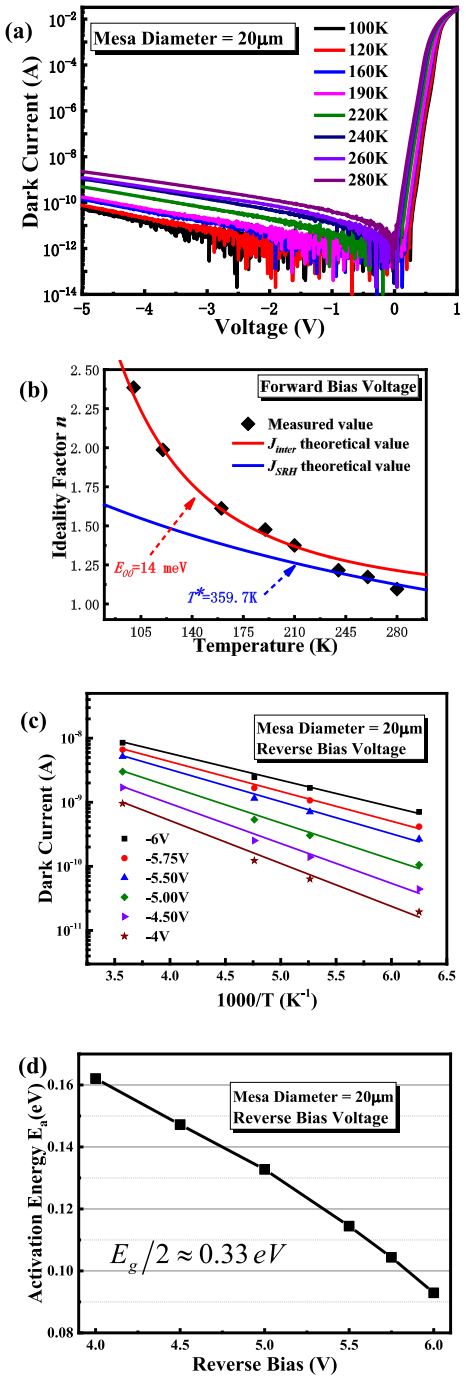

FIGURE 3. **(a) Dark current of 20-μm-diameter diode versus voltage at temperatures of 100 K, 120 K, 160 K, 190 K, 220 K, 240 K, 260 K and 280 K. (b) Ideality factor versus temperature (symbols). The red curve is a fitting with n_{trap}, where $E_{00} = 14$ meV, and blue line relates to n_{SRH} when $T^* = 359.7$ K. (c) Semi-logarithmic dark current versus $1000/T$ characteristics at various reverse voltages, where the activation energy E_a can be extracted. (d) E_a as a function of reverse bias. When the temperature is ≥240 K, the main dark current sources are diffusion and SRH processes. However, the trap-assisted-tunneling process is the major dark current source in the 100 K–220 K range.**

IV. RESPONSIVITY

The input light wavelengths are 850 nm, 1310 nm and 1550 nm, and the power ranges from 0 to 0.37 mW. The output currents were measured, with results as shown in Fig. 4(a), as functions of input optical power and wavelength indicated by hollow discrete points. The responsivity (R) is a key parameter for photodetectors. The output current (I_{output}) is a first-degree polynomial function of the effective input optical power (P_{input}), and the first-degree coefficient is R, i.e.,

$$I_{output} = R \cdot P_{input} + I_0 \tag{2}$$

Here, I_0 is the intercept current of the linear curve and is related to the noise and dark current of the device. The responsivity is the slope of the fitting curve of the output current versus the input optical power, as shown in Fig. 4(a). The measured responsivities are 0.518 A/W, 0.425 A/W and

0.249 A/W at 850 nm, 1310 nm and 1550 nm, respectively. The corresponding theoretical absorption efficiencies of our structure are thus 79.32%, 48.41% and 24.12%, respectively, as determined using the scattering matrix method [38]. The intercepts of the three linear fitting curves on the output current axis do not coincide, which may be explained by coupling and fiber loss errors or perturbation of the dark current at low incident powers.

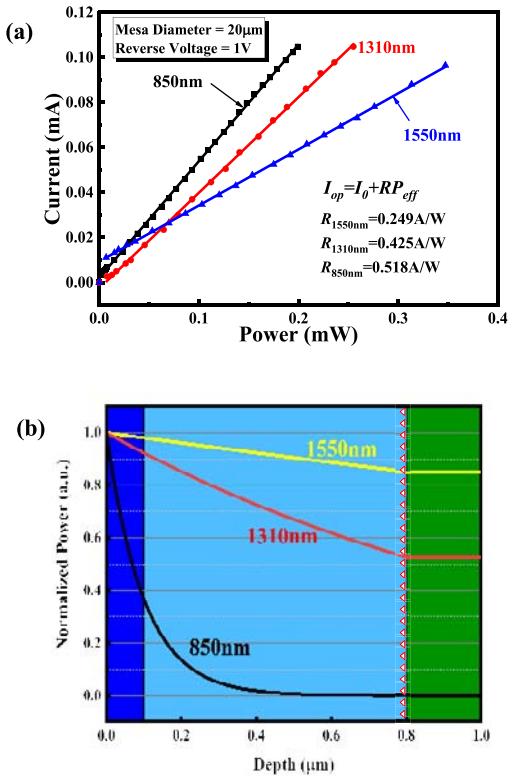

FIGURE 4. **(a) Output current versus incident power at 850 nm, 1310 nm and 1550 nm, with corresponding linear fitting based on expression (2). The responsivities are 0.518 A/W, 0.425 A/W and 0.249 A/W, respectively. (b) Theoretical power distributions of the input light at 850 nm, 1310 nm and 1550 nm versus light propagation depth.**

The theoretical input optical power distributions in the Ge layer at 850 nm, 1310 nm and 1550 nm are calculated by $P = P_0 \exp(-\alpha W)$, where the α is absorption coefficient, W is the light propagation depth and P_0 is the initial input optical power of Ge layer, as shown in Fig. 4(b). At 850 nm, the absorption length of the Ge material is 0.5 μm, which is lower than the Ge layer thickness in our devices [39], and the ratio of theoretical to measured responsivity is approximately 95.26%, which could represent the collection efficiency of the photon-generated carriers. Therefore, it can be concluded that the Si/Ge interface has little or no effect on the collection of the photo-generated carriers. However, at 1310 nm and 1550 nm, the absorption lengths are 1.25 μm and 3.33 μm, respectively, which are much greater than the Ge layer thickness. The responsivity ratios are 83.09% and 82.59%, respectively, which are lower than those at 850 nm, as shown in Table 1. This can be explained by the lower Ge absorption coefficient around the interface because of compressive stress around the interface because of the high dislocation density. Assuming that the 800 nm Ge layer was divided into a 750 nm regular bulk Ge layer and a 50 nm virtual interface Ge layer. The transfer matrix method was utilized to calculate the absorption coefficient of the virtual layer, and found that it is equal to 6100/cm at 1310 nm and 1500/cm at 1550 nm, lower than bulk Ge. Therefore, it is reasonable to infer that the Si/Ge interface could reduce the photon absorption efficiency around it [40]. In other words, the interface reduces the effective absorption coefficient but has little effect on the collection efficiency.

TABLE 1. **Summary of absorption coefficient data and calculations of responsivity for Ge bulk at 850 nm, 1310 nm and 1550 nm.**

Wavelength (nm)	*Absorption coefficient of Ge (μm^{-1})*	*Absorption length (μm)*	*Theoretical quantum efficiency*	*Theoretical responsivity(T) (A/W)*	*Measurement responsivity (M) (A/W)*	*Ratio (M/T)*
850	2	0.5	0.7932	0.5438	0.518	95.26%
1310	0.8	1.25	0.4841	0.5115	0.425	83.09%
1550	0.3	3.33	0.2412	0.3015	0.249	82.59%

V. BANDWIDTH

The bandwidth, i.e., the 3-dB-cutoff frequency (f_{3dB}), is another important parameter for photodetectors. In the photodetector bandwidth measurement experiments, the bandwidth is the 3-dB cutoff frequency of the S_{21} parameter determined using a vector network analyzer [41]. Therefore, the photodetector bandwidth (f_{3dB}) is actually the system cut-off frequency, which is limited by the photodetector's carrier transition time (f_t) and the resistor-capacitor RC delay (f_{RC}) of the system with load resistance (R_L):

$$f_{3dB} = \sqrt{\frac{1}{f_t^{-2} + f_{RC}^{-2}}} \tag{3}$$

Ideally, f_{RC} can be calculated using $f_{RC} = \frac{1}{2\pi(R_{pd}+R_L)C_{pd}} = \frac{4W_D}{2\pi(R_{pd}+R_L)\times\varepsilon\varepsilon_0\times\pi D^2}$, where C_{pd} and R_{pd} are the photodetector's capacitance and resistance, respectively, and R_L is 75 Ω [42]. Additionally, f_t is given by $2.4\ v_{av}/(2\pi W_D)$, where v_{av} is the average drift velocity (at −0.5 V bias, $v_{av} \approx 2.19 \times 10^5$ m/s) [43], and W_D is the depletion region thickness (here, $W_D = 0.7$ μm). The measured R_{pd} of our 20-μm-diameter devices is 8.05 Ω. Therefore, theoretically, the 3-dB bandwidth of the 20-μm-diameter device is 29.0 GHz, which is determined using the RC delay frequency (∼29.8 GHz).

The R&S ZNB 40 vector network analyzer was used to measure the 3-dB bandwidth, and results for 20-μm-diameter devices are shown in Fig. 5. The 3-dB cut-off frequency is 20.6 GHz at −0.5 V. At high frequencies, the carrier exchange between the defect states and the energy band was actually limited [44]. Therefore, the interface has a negligible effect on the high-frequency responses of Si/Ge photodiodes,

and the parasitic capacitances of the pad metal, mesa sidewall and the measurement system cause the bandwidth to be lower than the theoretical value [45].

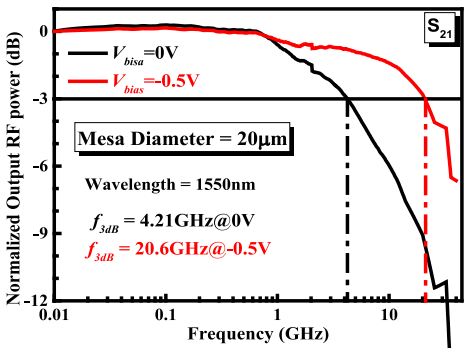

FIGURE 5. Frequency dependence of response. The 3-dB frequencies at 4.21 GHz and 20.6 GHz were extracted at zero bias and −0.5 V, respectively.

VI. CONCLUSION

In conclusion, in Ge-on-SOI photodiodes, carriers are considered to tunnel through the triangular barrier around the interface, meaning that trap-assisted tunneling enhances the dark current at low temperatures and a high reverse bias voltage. A characteristic tunneling energy of 14 meV was extracted at low temperature, which is related to a heavy effective mass of $18m_0$, indicating that high compressive strain occurs and a heavy-hole band arises around the Si/Ge interface. A characteristic distribution energy of $E* = 31$ meV was extracted at high temperature, which corresponds to a defect state density of $N_t(E) \propto \exp(2E/E^*)$, which follows a tail distribution. There are large differences between practice and theory in the responsivity performance, with ratios of 95.56%, 86.07% and 85.69% at 850 nm, 1310 nm and 1550 nm, respectively. This means that the Si/Ge interface would reduce the photon absorption efficiency or the lifetime of photo-generated carriers around it but has little effect on the collection efficiency. Additionally, the 3-dB-cut-off frequency was measured to be 20.9 GHz. Defects are believed to have little impact on the bandwidth at such high frequencies. Therefore, while Si/Ge interface states degrade the dark current and absorption, Ge remains one of the best choices for next-generation detectors to achieve high bandwidth detection.

REFERENCES

[1] J. Liu, "Monolithically integrated Ge-on-Si active photonics," *Photonics*, vol. 1, no. 3, pp. 162–197, 2014.
[2] M. Sakib *et al.*, "Demonstration of a 50 Gb/s all-silicon waveguide photodetector for photonic integration," in *Conf. Lasers Electro Opt. OSA Tech. Dig.*, 2018.
[3] J. S. Orcutt *et al.*, "Monolithic silicon photonics at 25 Gb/s," in *Opt. Fiber Commun. Conf. OSA Tech. Dig.*, 2016.
[4] D. Monroe, "Silicon photonics: Ready to go the distance?" *Commun. ACM*, vol. 59, no. 5, pp. 26–28, 2016.
[5] J. Endres, S. Danis, and G. Bauer, "The misfit dislocation density profile in graded SiGe/Si(001) layers prepared at different temperatures," *J. Phys. Condensed Matter*, vol. 25, no. 17, 2013, Art. no. 175802.
[6] H. Ye and J. Yu, "Germanium epitaxy on silicon," *Sci. Technol. Adv. Mater.*, vol. 15, no. 2, 2014, Art. no. 024601.
[7] T. A. Langdo *et al.*, "High quality Ge on Si by epitaxial necking," *Appl. Phys. Lett.*, vol. 76, no. 25, pp. 3700–3702, 2000.
[8] S. Klinger, M. Berroth, M. Kaschel, M. Oehme, and E. Kasper, "Ge-on-Si p-i-n photodiodes with a 3-dB bandwidth of 49 GHz," *IEEE Photon. Technol. Lett.*, vol. 21, no. 13, pp. 920–922, Jul. 2009.
[9] S. J. Koester *et al.*, "Ge-on-SOI-detector/Si-CMOS-amplifier receivers for high-performance optical-communication applications," *J. Lightw. Technol.*, vol. 25, no. 1, pp. 46–57, Jan. 26, 2007.
[10] Y. Kang *et al.*, "Monolithic germanium/silicon avalanche photodiodes with 340 GHz gain-bandwidth product," *Nat. Photon.*, vol. 3, no. 1, pp. 59–63, 2009.
[11] J. Michel, J. Liu, and L. C. Kimerling, "High-performance Ge-on-Si photodetectors," *Nat. Photon.*, vol. 4, no. 8, pp. 527–534, 2010.
[12] Y. Zhang *et al.*, "A high-responsivity photodetector absent metal-germanium direct contact," *Opt. Exp.*, vol. 22, no. 9, pp. 11367–11375, 2014.
[13] L. Virot *et al.*, "Germanium avalanche receiver for low power interconnects," *Nat. Commun.*, vol. 5, p. 4957, Sep. 2014.
[14] C.-K. Tseng *et al.*, "A self-assembled microbonded germanium/silicon heterojunction photodiode for 25 Gb/s high-speed optical interconnects," *Sci. Rep.*, vol. 3, p. 3225, Nov. 2013.
[15] Y. Miyasaka *et al.*, "Ge/graded-SiGe multiplication layers for low-voltage and low-noise Ge avalanche photodiodes on Si," *Jpn. J. Appl. Phys.*, vol. 55, no. 4, 2016, Art. no. 04EH10.
[16] H. Cong *et al.*, "Silicon based GeSn p-i-n photodetector for SWIR detection," *IEEE Photon. J.*, vol. 8, no. 5, Oct. 2016, Art. no. 6804706.
[17] S. Su *et al.*, "GeSn p-i-n photodetector for all telecommunication bands detection," *Opt. Exp.*, vol. 19, no. 7, pp. 6400–6405, 2011.
[18] J. Shim *et al.*, "Germanium p-i-n avalanche photodetector fabricated by point defect healing process," *Opt. Lett.*, vol. 39, no. 14, pp. 4204–4207, 2014.
[19] I. G. Kim *et al.*, "High-performance photoreceivers based on vertical-illumination type Ge-on-Si photodetectors operating up to 43 Gb/s at λ∼1550nm," *Opt. Exp.*, vol. 21, no. 25, pp. 30716–30723, 2013.
[20] H. Chen *et al.*, "−1 V bias 67 GHz bandwidth Si-contacted germanium waveguide p-i-n photodetector for optical links at 56 Gbps and beyond," *Opt. Exp.*, vol. 24, no. 5, pp. 4622–4631, 2016.
[21] D. Zhang *et al.*, "High-responsivity GeSn short-wave infrared p-i-n photodetectors," *Appl. Phys. Lett.*, vol. 102, no. 14, 2013, Art. no. 141111.
[22] L. E. Vorobyev, *Handbook Series on Semiconductor Parameters*, vol. 1. Singapore: World Sci., 1996 pp. 33–57.
[23] M. S. Alam, M. S. Rahman, M. R. Islam, A. G. Bhuiyan, and M. Yamada, "Refractive index, absorption coefficient, and photoelastic constant: Key parameters of InGaAs material relevant to InGaAs-based device performance," in *Proc. IEEE Int. Conf. Indium Phosphide Related Mater.*, 2007, pp. 343–346.
[24] C. Li *et al.*, "High bandwidth surface-illuminated InGaAs/InP uni-travelling-carrier photodetector," *Chin. Phys. B*, vol. 22, no. 11, 2013, Art. no. 118503.
[25] C. Li *et al.*, "High-bandwidth and high-responsivity top-illuminated germanium photodiodes for optical interconnection," *IEEE Trans. Electron Devices*, vol. 60, no. 3, pp. 1183–1187, Mar. 2013.
[26] S. R. Forrest, R. F. Leheny, R. E. Nahory, and M. A. Pollack, "$In_{0.53}Ga_{0.47}As$ photodiodes with dark current limited by generation-recombination and tunneling," *Appl. Phys. Lett.*, vol. 37, no. 3, pp. 322–325, 1980.
[27] A. Sellai, "Temperature dependence of dark current in a Si-pin photodiode," in *Proc. IEEE Int. Conf. Semicond. Electron.*, 2008, pp. 267–270.
[28] P. Dalapati, N. B. Manik, and A. N. Basu, "Influence of temperature on tunneling-enhanced recombination in Si based p-i-n photodiodes," *J. Semicond.*, vol. 35, no. 8, 2014, Art. no. 082001.
[29] A. Czerwinski, E. Simoen, A. Poyai, and C. Claeys, "Activation energy analysis as a tool for extraction and investigation of p-n junction leakage current components," *J. Appl. Phys.*, vol. 94, no. 2, pp. 1218–1221, 2003.
[30] A. Rogalski, *Infrared Detectors*. Amsterdam, The Netherlands: Gordon Breach Sci., 2000.
[31] E. Simoen, C. Claeys, A. Czerwinski, and J. Katcki, "Accurate extraction of the diffusion current in silicon p-n junction diodes," *Appl. Phys. Lett.*, vol. 72, no. 9, pp. 1054–1056, 1998.

[32] T. Walter, R. Herberholz, and H. W. Schock, "Distribution of defects in polycrytalline chalcopyrite thin films," *Solid-State Phenom.*, vols. 51–52, no. 5, p. 309, 1996.
[33] L. Colace, M. Balbi, V. Sorianello, and G. J. Assanto, "Temperature-dependence of Ge on Si p–i–n photodetectors," *Lightw. Tech.*, vol. 26, no. 14, pp. 2211–2214, Jul. 15, 2008.
[34] K.-W. Ang, J. W. Ng, G.-Q. Lo, and D.-L. Kwong, "Impact of field-enhanced band-traps-band tunneling on the dark current generation in germanium p-i-n photodetector," *Appl. Phys. Lett.*, vol. 94, no. 22, 2009, Art. no. 223515.
[35] X. Li, J. Zhao, H. Lu, J. Fang, and Y. Xia, "Forward-tunneling current voltage characteristics of HgCdTe p-on-n photodiodes," in *Proc. SPIE*, vol. 3379. Orlando, FL, USA, 1998, pp. 601–617.
[36] F. A. Padovani and R. Stratton, "Field and thermionic-field emission in Schottky barriers," *Solid-State Electron.*, vol. 9, no. 7, pp. 695–707, 1966.
[37] A. Jasenek, U. Rau, V. Nadenau, and H. W. Schock, "Electronic properties of $CuGaSe_2$-based heterojunction solar cells. Part II. Defect spectroscopy," *J. Appl. Phys.*, vol. 87, no. 1, pp. 594–602, 2000.
[38] L. Chong *et al.*, "High-responsivity vertical-illumination Si/Ge uni-traveling-carrier photodiodes based on silicon-on-insulator substrate," *Sci. Rep.*, vol. 6, no. 1, 2016, Art. no. 27743.
[39] W. C. Dash and R. Newman, "Intrinsic optical absorption in single-crystal germanium and silicon at 77°K and 300°K," *Phys. Rev.*, vol. 99, no. 4, pp. 1151–1155, 1955.
[40] V. Srikant and D. R. Clarke, "Optical absorption edge of ZnO thin films: The effect of substrate," *J. Appl. Phys.*, vol. 81, no. 9, pp. 6357–6364, 1997.
[41] *Vector Network Analyzers User Manual*, R&S ZNB/ZNBT, München, Germany, 2015, pp. 1244–1280.
[42] R. A. Aroca, and S. P. Voinigescu, "A large swing, 40-Gb/s SiGe BiCMOS driver with adjustable pre-emphasis for data transmission over 75 Ω coaxial cable," in *Proc. Compd. Semicond. Integr. Circuit Symp.*, vol. 43, 2007, pp. 2177–2186.
[43] M. Levinshtein, S. Rumyantsev, and M. Shur, *Handbook Series on Semiconductor Parameters*, vol. 1. Singapore: World Sci., 1996, pp. 33–56.
[44] M. Hanzaz, A. Bouhdada, P. Gibart, and F. Omnes, "Impact of the defects on the electrical and optical properties of AlGaN ultraviolet photodetectors," *J. Appl. Phys.*, vol. 92, no. 1, pp. 13–18, 2002.
[45] J. S. Choi and G. W. Neudeck, "Frequency-dependent capacitance-voltage characteristics for amorphous silicon-based metal-insulator-semiconductor structures," *IEEE Trans. Electron Devices*, vol. 39, no. 11, pp. 2515–2522, Nov. 1992.

CHONG LI received the Bachelor of Engineering degree in electronics science and technology from the Beijing Institute of Technology and the Ph.D. degree in microelectronics and solid state electronics from the Institute of Semiconductors, Chinese Academy of Sciences. In 2014, he joined the Beijing University of Technology, China. Her interests include the high speed silicon-based photodiodes and high sensitivity avalanche photodiodes.

BEN LI received the B.S. degree in electronics science and technology from the Beijing University of Technology, Beijing, China, in 2015, where he is currently pursuing the M.S. degree. His current research interests include Ge/Si photodiodes and InGaAs/InP photodiodes.

SHIHONG QIN received the B.S. degree in integrated circuit design and integration system from Huaqiao University, Xiamen, China, in 2015. He is currently pursuing the M.S. degree with the Beijing University of Technology, Beijing, China. His current research interest includes grating-coupling high-speed Si photodiodes.

JIALE SU received the B.S. degree in electronic science and technology from Shandong Technology and Business University, Yantai, China, in 2017. She is currently pursuing the M.S. degree with the Beijing University of Technology, Beijing, China. Her current research interest includes graphene modulator.

XIAOYING HE was born in Hubei, China, in 1981. She received the B.S. degree in physics from Hubei Normal University and the M.S. and Ph.D. degrees from the Huazhong University of Science and Technology in 2006 and 2009, respectively.

From 2005 to 2006, she was with Accelink Technology Company Ltd., Wuhan, China. From 2007 to 2008, she was a Research Assistant with the Hong Kong Polytechnic University. From 2009 to 2012, she was a Post-Doctoral Research Fellow with Hong Kong Polytechnic University. She has been with Fudan University as a Lecturer and an Associate Professor with the Department of Optical Science and Technology since 2012 and 2014, respectively. In 2017, she is appointed as a Professor with the Beijing University of Technology. Her main research interests are semiconductor optoelectronic devices, graphene optoelectronic devices, fiber laser, optical fiber sensors, and optical design.

XIA GUO was born in Shandong, China, in 1974. She received the Ph.D. degree in semiconductors optoelectronic devices from the Beijing University of Technology, Beijing, China, in 2003. He is currently a Professor with the School of Electronic Engineering, Beijing University of Posts and Telecommunications, China. His current research interests include high-response and high-speed PiN diodes in Si, high speed VCSELs in GaAs, and ultrahigh-sensitive photodiodes in graphene.